JCB Report

Regulation of limb patterning by extracellular microfibrils

Emilio Arteaga-Solis,[1] Barbara Gayraud,[1] Sui Y. Lee,[1] Lillian Shum,[2] Lynn Sakai,[3] and Francesco Ramirez[1]

[1]Brookdale Center, Department of Biochemistry and Molecular Biology, Mount Sinai School of Medicine, New York, NY 10029
[2]Craniofacial Development Section, National Institute of Arthritis and Musculoskeletal and Skin Diseases, National Institutes of Health, Bethesda, MD 20892
[3]The Shriners Hospital for Children, Portland, OR 97201

To elucidate the contribution of the extracellular microfibril–elastic fiber network to vertebrate organogenesis, we generated fibrillin 2 (*Fbn2*)–null mice by gene targeting and identified a limb-patterning defect in the form of bilateral syndactyly. Digit fusion involves both soft and hard tissues, and is associated with reduced apoptosis at affected sites. Two lines of evidence suggest that syndactily is primarily due to defective mesenchyme differentiation, rather than reduced apoptosis of interdigital tissue. First, fusion occurs before appearance of interdigital cell death; second, interdigital tissues having incomplete separation fail to respond to apoptotic clues from implanted BMP-4 beads. Syndactyly is associated with a disorganized matrix, but with normal BMP gene expression. On the other hand, mice double heterozygous for null *Fbn2* and *Bmp7* alleles display the combined digit phenotype of both nullizygotes. Together, these results imply functional interaction between Fbn2-rich microfibrils and BMP-7 signaling. As such, they uncover an unexpected relationship between the insoluble matrix and soluble factors during limb patterning. We also demonstrate that the *Fbn2*-null mutation is allelic to the recessive shaker-with-syndactyly (*sy*) locus on chromosome 18.

Introduction

Limb patterning is controlled by complex interactions of four signaling centers that promote establishment of the main axes, growth, and cell differentiation (Johnson and Tabin, 1997; Tickle, 1999). The apical ectodermal ridge and the underlying progress zone regulate proximal-distal outgrowth of the limb bud, and proliferation of undifferentiated mesenchyme, respectively. During the late phase of limb morphogenesis, rays of condensing mesenchyme appear in the distal region of the bud (autopod); they grow and differentiate into cartilage (digits), whereas interposed tissues (interdigits) undergo programmed cell death. Therefore, digit formation is the combined result of chondrogenic outgrowth and interdigital cell death. In turn, the choice of autopodial mesoderm to undergo either chondrogenesis or apoptosis is primarily determined by positional information established earlier in ontogeny. At least three bone morphogenetic proteins (BMPs),* BMP-2, BMP-4, and BMP-7, have been implicated in specifying the chondrogenic and apoptotic fate, and in regulating digit identity (Hogan, 1996; Dahna and Fallon, 2000). In spite of much effort, the mechanism responsible for the distinct actions of BMP signaling in the autopod remains largely unknown. Conceivably, it may involve different types of BMP receptors, formation of functionally distinct dimers, interactions with local soluble factors, and dynamic clues from surrounding tissues (Hogan, 1996; Merino et al., 1998, 1999; Tang et al., 2000). There is also increasing evidence for the involvement of extracellular proteoglycans and proteases in modulating growth factor activity (Christian, 2000).

The extracellular matrix consists of a highly heterogeneous mixture of insoluble and soluble molecules that orchestrate a variety of cellular processes and developmental programs. Extracellular microfibrils, alone or associated with elastin in the elastic fiber, confer critical properties to the connective tissue of the developing and adult organism (Ramirez, 1996). Microfibril–elastic fiber networks vary greatly in length, thickness, and tridimensional organization in order to accommodate the strength and direction of mechanical forces experienced by individual tissues (Mecham and Davis, 1994). It is widely believed that the morphological diversification of the insoluble matrix may also reflect nonstructural roles. For example, transient appearance of an elastic scaffold in the limb bud of the chick embryo was interpreted to sug-

Address correspondence to Francesco Ramirez, Department of Biochemistry and Molecular Biology, Mount Sinai School of Medicine, One Gustave L. Levy Place, Box 1020, New York, NY 10029. Tel.: (212) 241-1757. Fax: (212) 722-5999. E-mail: ramirf01@doc.mssm.edu

*Abbreviations used in this paper: BMP, bone morphogenetic protein; CCA, congenital contractural arachnodactyly; ES, embryonic stem; Fbn, fibrillin; *sy*, shaker-with-syndactyly; TUNEL, Tdt-mediated dUTP nick end labeling.

Key words: BMP; fibrillin; limb patterning; morphogenesis; syndactyly

gest that this specialized matrix may physically delineate the location and size of cartilaginous structures (Hurlé et al., 1994). Indeed, ectopic stimulation of chondrogenesis at interdigital sites was shown to be preceded by disruption of the elastic scaffold and substantial matrix reorganization (Hurlé et al., 1994). However, the role of extracellular macroaggregates in demarcating specific areas in developing tissues has never been formally or genetically proven.

Another evolving concept is that the insoluble matrix may also modulate intercellular signaling by guiding the diffusion, sequestration, activation, or presentation of soluble factors to the surrounding cells (Flaumenhaft and Rifkin, 1991). A case in point is the postulated regulation by microfibrils of transforming growth factor-β activity through binding of the large latent complex (Taipale and Keski-Oja, 1997). The glycoproteins fibrillin 1 (Fbn1) and fibrillin 2 (Fbn2) are the major, if not the only, structural components of extracellular microfibrils (Handford et al., 2000). *Fbn* gene expression and microfibrillar deposition precede elastic fiber formation, which in most tissues occurs between midgestation and early postnatal life (Mecham and Davis, 1994). Mutations in the human *Fbn1* and *Fbn2* genes are responsible for the pleiotropic manifestations of Marfan syndrome and the transient phenotype of congenital contractural arachnodactyly (CCA), respectively (Ramirez, 1996). Mice harboring targeted mutations in the *Fbn1* gene have demonstrated that Marfan syndrome severity is determined by the degree of functional impairment of extracellular microfibrils (Pereira et al., 1997, 1999; Gayraud et al., 2000). Moreover, the longer bones of *Fbn1*-deficient mice lend credence to the hypothesis that microfibrils play a role in skeletal development (Pereira et al., 1999).

In contrast to the emerging information about Fbn1 biology, little is known about the role of Fbn2 during embryonic development. Here we report the creation of a null allele of the mouse *Fbn2* gene. Mutant homozygotes recapitulate the human CCA phenotype, and also display bilateral syndactyly of forelimbs and hindlimbs. The patterning abnormality appears early in autopod formation, and before apoptotic cells are observed in the interdigital tissues. We show that Fbn2 deficiency is associated with disorganized microfibrils, and provide genetic evidence for interaction between Fbn2 and BMP-7. Altogether, the results demonstrate for the first time that specific intercellular signaling events during limb morphogenesis depend on proper supramolecular assembly of the insoluble extracellular matrix.

Results and discussion

Generation of Fbn2$^{-/-}$mice

To create a null *Fbn2* allele, the 1.2-kb region encompassing exon 1 was replaced by the pGK-*neo* cassette (Fig. 1 a). Exon 1 contains the 5′ untranslated region of the mRNA, in addition to coding for the signal peptide and the first 85 amino acids of the protein (Zhang et al., 1995). After electroporation of the targeting vector and selection of G418-resistant embryonic stem (ES) clones carrying the recombinant allele (Fig. 1 b), three chimeric animals were generated and germ line transmission of the mutant allele was demonstrated in one of them by Southern hybridization (Fig. 1 c). Northern analysis of newborn lung RNA, and Western analysis of conditioned media from fibroblast cultures documented loss of *Fbn2* gene activity in homozygous mutant animals (Fig. 1, d and e).

Mating of heterozygous mutant animals led to the production of *Fbn2*$^{-/-}$ mice in the pure (129/Sv) and hybrid (C57Bl/6Jx129/Sv) genetic backgrounds. Heterozygous and homozygous mutant mice were born at the expected frequency, and were viable and fertile. Examination of newborn *Fbn2*$^{-/-}$ mice revealed contractures of carpal, metacarpal, and phalangeal joints in the forelimbs (Fig. 2 a); upon mechanical extension, the large joints of the hindlimbs were felt to be stiffer than those of wild-type littermates. As with CCA patients (Ramirez, 1996), contractures in *Fbn2*-deficient mice disappeared within the first few days of postnatal life. The presence of contractures in heterozygous CCA patients and in homozygous mice indicates a pathogenic equivalency between dominant-negative and loss-of-function mutations of Fbn2.

Limb skeletal abnormalities

Examination of *Fbn2*-deficient mice identified an additional unexpected trait, bilateral syndactily, indicative of a morphogenetic role of the extracellular protein (Fig. 2 b). The phenotype is fully penetrant and shows variable expression in different backgrounds, suggestive of genetic modifier(s) (Table I). Complete fusion or close apposition of chondrogenic elements of the central two or three digits (digits 2–4) was observed in both forelimbs and hindlimbs (Table I). Syndactyly always involves the first phalange, thus suggesting that the perturbation occurs early during proximal-distal outgrowth of the autopod (Fig. 2 b). This postulate was corroborated by the finding of malformed autopods in mutant embryos before the appearance of interdigital cell death (Fig. 2 c) (Chen and Zhao, 1998). It was also confirmed experimentally by comparing the effect of exogenous BMP administration to interdigital rays of mutant and wild-type embryos (Fig. 2 d). Implantation of latex beads loaded with BMP-2, BMP-4, or BMP-7 into chick interdigital tissues has been shown to induce *Msx* gene expression and precocious cell death (Ganan et al., 1996, 1998; Macias et al., 1997; Merino et al., 1998). Increased expression of *Msx1* and *Msx2* genes in response to local BMP-4 administration was indeed observed in wild-type interdigital tissues, as well as in unaffected regions of *Fbn2* mutant interdigital rays (Fig. 2 d). In contrast, there was no significant increase of *Msx* gene activity around BMP-4 beads implanted into mutant interdigital tissues having incomplete separation (Fig. 2 d). It should be noted that the data shown in Fig. 2 d were obtained with mutant limbs incubated for a longer period than wild-type autopod, in order to maximize the effect of the implanted beads. Accumulation of *Msx* transcripts at the tip of the autopod is consistent with the normal pattern of gene expression during limb development (see below and Fig. 2 e). Altogether, the data strongly suggest that *Fbn2* deficiency negatively affects promotion of mesenchyme differentiation during early autopod morphogenesis, rather than subsequent interdigital apoptosis. The precise cellular lesion (i.e., commitment vs. proliferation of presumptive interdigital cells) remains to be determined. At variance with previous antisense interference experiments in rat organ cultures,

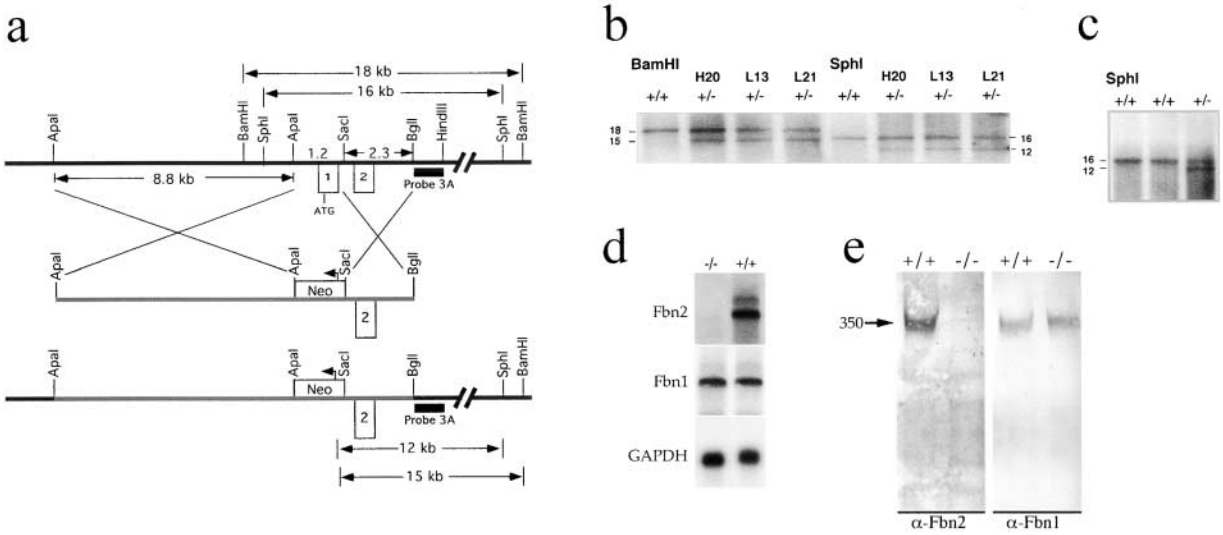

Figure 1. **Schematic illustration of *Fbn2* gene targeting.** (a) From top to bottom: restriction map of the targeted genomic region which indicates the relative positions of exons 1 and 2 (□) and probe 3 A (■), as well as the sizes of relevant DNA fragments; targeting vector with the arrow signifying the transcriptional orientation of the *neo* gene (□); null *Fbn2* allele with the predicted sizes of mutant BamHI and SphI fragments. (b) Southern hybridization of BamHI and SphI-digested DNA from wild-type (+/+) and correctly targeted (+/−) ES clones. (c) Southern hybridization of SphI-digested tail DNA from the chimeric progeny demonstrating germ line transmission of the *Fbn2* mutation in one animal (+/−). (d) Northern hybridizations to *Fbn1*, *Fbn2*, and GAPDH of RNA from wild-type (+/+) and mutant (−/−) newborn lungs. (e) Western analysis of conditioned media from wild-type (+/+) and mutant (−/−) primary fibroblast cultures with antibodies against Fbn1 and 2 (α-Fbn1 and α-Fbn2); size of the fibrillins (350 kD, arrow) was estimated against the migration of protein standards (not shown).

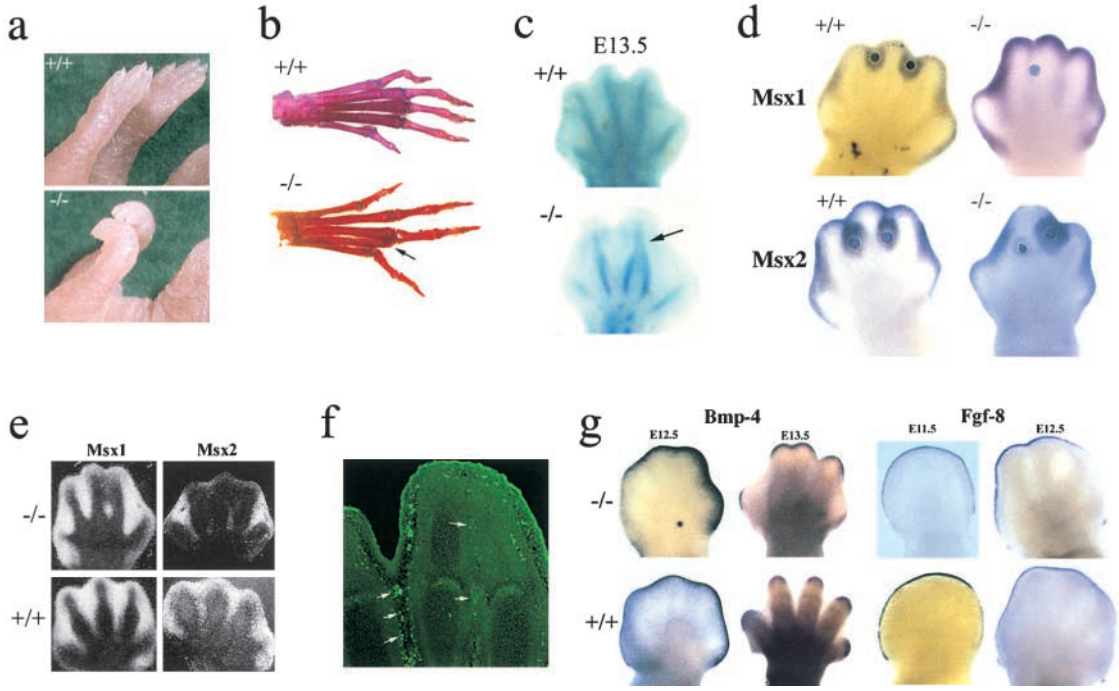

Figure 2. **Analysis of *Fbn2* mutant limbs.** (a) Forelimbs of wild-type (+/+) and mutant (−/−) newborn mice showing contractures of the wrist and metacarpal joints. (b) Skeletal preparation of adult hindlimbs of wild-type (+/+) and mutant (−/−) mice with arrow pointing to hard tissue syndactily in the latter. (c) Staining of cartilaginous elements of E13.5 hindlimbs of wild-type (+/+) and mutant (−/−) embryos with arrow pointing to digit fusion in the latter. (d) Whole-mount hybridizations to *Msx* probes of E13.5 wild-type (+/+) and mutant (−/−) hindlimbs with implanted BMP-4–coated beads. (e) In situ hybridizations to *Msx* probes of wild-type (+/+) and mutant (−/−) E13.5 hindlimbs. (f) In situ TUNEL assay of E13.5 *Fbn2*$^{-/-}$ hindlimb with arrows pointing to apoptotic signals; note the fewer number of dying cells in the interdigital region destined to fuse, compared with the interdigital ray that will regress and lead to digit separation. (g) Whole-mount in situ hybridizations to *Bpm-4* and *Fgf-8* of E11.5-E13.5 hindlimbs of wild-type (+/+) and mutant (−/−) embryos.

we did not find evidence of impaired branching morphogenesis in *Fbn2*$^{-/-}$ lungs (Yang et al., 1999). This discrepancy may reflect the contribution of additional cellular factors present in vivo and absent in isolated organ cultures.

Fbn2 deficiency is associated with reduced apoptosis of interdigital tissue

BMP activation of programmed cell death correlates with induction of *Msx* gene expression (Marazzi et al., 1997). Accordingly, we analyzed expression of *Msx* genes in *Fbn2* mutant autopods. We also examined expression of genes coding for regulators of autopod morphogenesis, including *Fgf-8*, a major signaling molecule secreted by the apical ectodermal ridge during proximal-dorsal limb outgrowth, and *Bmp-4*, a representative of BMPs involved in digit formation (Hogan, 1996; Johnson and Tabin, 1997; Tickle, 1999). Consistent with digit fusion, there was no detectable *Msx* expression in the affected regions of mutant interdigital rays (Fig. 2 e). Histological analyses using the Tdt-mediated dUTP nick end labeling (TUNEL) assay corroborated this finding. Visualization of apoptotic signals in the interdigital rays of mutant embryos did in fact document the presence of fewer dying cells in affected compared with unaffected tissues (Fig. 2 f). Consistent with the notion that the mutation affects early morphogenesis, apoptosis is impaired but not abolished by loss of Fbn2. In contrast to the *Msx* genes, neither *Fgf-8* nor *Bmp-4* are abnormally expressed in mutant autopods (Fig. 2 g). Normal *Bmp* gene expression in the presence of reduced apoptosis raised the possibility that alterations of the autopodial matrix may perturb sequestration and/or activation of intercellular signaling molecules.

Fbn2 deficiency alters microfibrillar organization and BMP signaling

Two distinct experiments were performed to validate the above hypothesis. In the first, we examined the morphology of microfibrillar aggregates during autopod development. Analysis of *Fbn1* and *Fbn2* expression documented that both transcripts accumulate predominantly, but not exclusively, in the interdigital rays (Fig. 3 a). Indirect immunofluorescence using specific antisera for Fbn1 and Fbn2 proteins, as well as for the cartilage-specific type II collagen, provided an overview of the arrangement of these extracellular macroaggregates in the wild-type and mutant autopods (Fig. 3 b). Whereas the Fbn-rich network of the wild-type embryo is distinctly arranged in the digital and interdigital rays (Fig. 3 b, top), that of the mutant is significantly disorganized with little or no Fbn immunoreactivity in the interdigital rays (Fig. 3 b, bottom). This last finding implies that Fbn2 is required for proper microfibrillar assembly; the requirement is tissue specific, in that networks of other organs are morphologically normal (Fig. 3 c).

The second test was designed to assess whether a functional connection exists between Fbn2 and BMP-7, one of the soluble regulators of digit formation (Hogan, 1996; Tickle 1999). To this end, we generated a compound heterozygous for *Fbn2*- and *Bmp-7*–null alleles. Whereas heterozygous *Bmp-7*–null mice are viable and morphologically normal, homozygotes die soon after birth and display several developmental abnormalities, including polydactily (Dudley et al., 1995; Luo et al., 1995). Analysis of *Fbn2*$^{+/-}$/*Bmp-7*$^{+/-}$ mice revealed a limb phenotype that combines the patterning defects (syndactyly and polydactyly) of each nullyzgous mouse (Fig. 4 a). Appearance of the null phenotype in the presence of half of the normal complement of each gene product implies functional interaction between the two proteins. This interaction in turn demonstrates that Fbn2 and BMP-7 are part of the same genetic program that regulates digit formation during autopod development.

Fbn2-null mutation is allelic to the sy locus on chromosome 18

There are several naturally occurring and artificially generated mutations in mice that affect limb development and patterning. One such mutation is the radiation-induced recessive locus shaker-with-syndactyly (*sy*), which is located on the same region of chromosome 18, where *Fbn2* resides (Hertwig, 1942; Lane et al., 1981; Li et al., 1993). Spontaneous mutations at the *sy* locus (*sy*^{fp} and *sy*$^{fp\text{-}2}$) that are viable in homozygosity and that only exhibit syndactyly have been described previously (Lane and Hummel, 1973; Sweet, 1996). Recent genomic analyses have suggested that *sy* is a multigene deletion of ~1 cM (Johnson et al., 1998). Hybridization of *sy* DNA to *Fbn2* probes demonstrated that the deletion includes the whole gene (unpublished data). Generation of double *Fbn2*$^{-/+}$/*sy*$^{fp/+}$ heterozygotes revealed that they exhibit the same bilateral syndactyly as *Fbn2*$^{-/-}$or *sy*^{fp}/*sy*^{fp} mice. Sequencing of RT-PCR products covering the entire *Fbn2* transcript from homozygous *sy*^{fp} mice identified a frameshift mutation that introduces an early termination codon at amino acid 1728, which is expected to destabilize the

Table I. **Morphological analysis of limbs from neonatal mutant mice**

		Forelimbs				Hindlimbs			
		Right		Left		Right		Left	
Background	Syndactyly digits	Soft tissue	Hard tissue	Soft tissue	Hard tissue	Soft tissue	Hard tissue	Soft tissue	Hard tissue
C57Bl/6Jx129sv	2, 3	9	0	9	0	12	1	8	5
(n = 54)	3, 4	13	1	12	1	4	14	4	19
	2, 3, 4	2	0	5	0	22	1	17	1
129sv	2, 3	0	0	0	0	1	1	0	0
(n = 31)	3, 4	19	0	19	0	4	5	2	7
	2, 3, 4	0	0	0	0	20	0	20	3

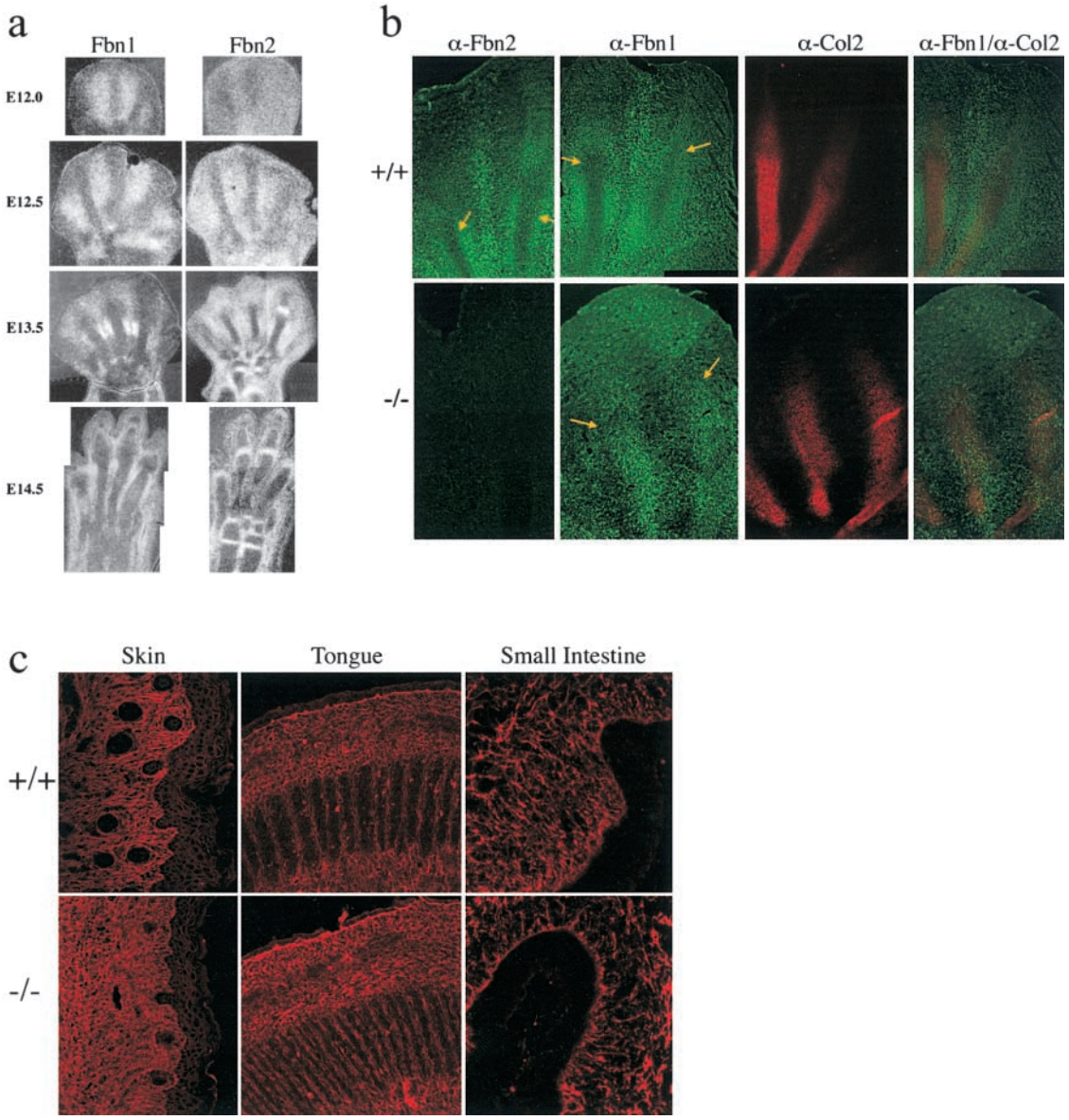

Figure 3. **Fbn expression and microfibrillar morphology in mutant *Fbn2* mice.** (a) In situ hybridization to *Fbn1* and *Fbn2* probes of E12.0-14.5 hindlimbs of wild-type (+/+) and mutant (−/−) embryos. (b) Immunofluorescence of wild-type (+/+) and mutant (−/−) E13.5 hindlimbs with antibodies against Fbn1 (α-Fbn1), Fbn2 (α-Fbn2), and type II collagen (α-Col 2). Arrows in Fbn-immunostained samples point to the developing digital (chondrogenic) rays that are intensively stained by the type II collagen antibody. Note the distinct organization of the microfibrillar network in the interdigital and digital rays of the wild-type autopod that is lost in the mutant samples. The disorganized architecture of the mutant matrix can be best appreciated in the superimposition of the α-Fbn1 and α-Col2 images. (c) Immunofluorescence of E13.5 skin, tongue, and small intestine from wild-type (+/+) and mutant (−/−) embryos.

mRNA. Northern and Western analyses confirmed this last postulate by documenting absence *Fbn2* mRNA and protein in sy^{fp}/sy^{fp} samples, respectively. (Fig. 4, b and c). Hence, loss of function of Fbn2 is the genetic lesion causing syndactyly in the contiguous gene deletion syndrome of the *sy* mouse.

Summary

This study identifies Fbn2 as the first insoluble matrix component to regulate limb patterning. This conclusion is based on two lines of evidence. First, altered microfibrillar morphology in mutant autopods implies a causal relationship between the organization of the insoluble macroaggregate and the patterning defect. Second, defective digit morphogenesis in double heterozygous $Fbn2^{+/-}/Bmp7^{+/-}$ mice indicates functional interaction between the matrix component and the growth factor. Hence, interactions with the microfibrillar network apparently control the distribution and/or activity of intercellular signals in the developing limb. The effect is highly specific in that it is restricted to a specific tissue and morphogenetic program.

A variety of extracellular modulators are known to be involved in intercellular signaling, including extracellular proteins that control signal availability, such as proteoglycans and tissue proteases (Christian, 2000). To the best of our knowledge, this is the first instance in which evidence has been presented for the involvement of an insoluble matrix macroag-

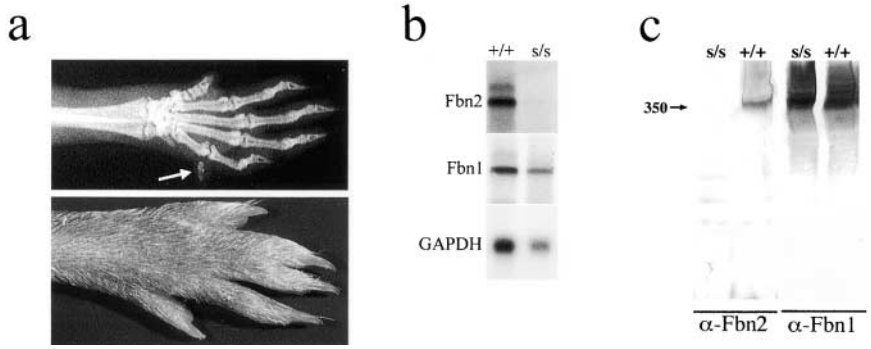

Figure 4. **Analysis of *Fbn2*$^{+/-}$/Bmp-7$^{+/-}$ and *sy*^{fp}/*sy*^{fp} mice.** (a) Limb patterning defects in double heterozygous *Fbn2*/*Bmp-7*–null mice. The x-ray on top shows an extra digit, whereas the picture at the bottom documents soft tissue syndactily in adult hindlimbs. (b) Northern hybridization of RNA from wild-type (+/+) and *sy*^{fp}/*sy*^{fp} (s/s) newborn mice. (c) Western analysis of conditioned media from wild type (+/+) and *sy*^{fp}/*sy*^{fp} (s/s) primary fibroblast cultures; size of fibrillins (350 kD, arrow) was estimated against the migration of protein standards (not shown).

gregate in the control of a specific patterning event. Thus more generally, the insoluble matrix may provide the structural scaffold that arranges morphogenetic clues in the intercellular space of the developing organism. This function could be exerted by binding directly to inactive growth factors (such as in the case of the latent transforming growth factor-β complex), indirectly through interaction with other matrix components (such as proteoglycans), or by a combination of both mechanisms (Flaumenhaft and Rifkin, 1991; Taipale and Keski-Oja, 1997). Irrespectively, our study demonstrates that the tridimensional organization of insoluble extracellular macroaggregates is critically important in establishing morphogenetic gradients during vertebrate embryogenesis.

Materials and methods

Gene targeting and mouse lines

The *Fbn2* targeting vector was engineered according to the gene replacement strategy outlined in Fig. 1 a. The 8.8-kb ApaI genomic fragment lying 5′ of exon 1 of *Fbn2,* was subcloned in the pBluescript SK(+/−) vector (Stratagene). The 2.3-kb SacI-BglI fragment extending 3′ of exon 1 and including exon 2, was then ligated into the blunt-ended NotI site. Finally, the 1.8-kb SalI-XhoI fragment from pGEM7(KJ1) plasmid containing the neomycin resistance gene (pGK-*neo*), was inserted into the XhoI site located between the homology regions and opposite of *Fbn2* transcription. The targeting construct was electroporated into ES cells that were selected as described previously (Pereira et al., 1997, 1999). Southern blots were performed with a probe outside of the homology region (probe 3 A) that recognizes 16-kb wild-type and 1-kb mutant bands in BamHI-digested DNA, as well as 14-kb wild-type and 11.5-kb mutant bands in SphI-digested DNA (Fig. 1 a). Chimeric animals were generated in the Mouse Genetics Shared Research Facility (Mount Sinai School of Medicine, New York, NY) according to the previously published protocol (Pereira et al., 1997, 1999). After germ line transmission, the *Fbn2* mutation was maintained in the hybrid (C57Bl/6Jx129/Sv) and pure (129/Sv) genetic background. The *sy*$^{fp/+}$ mouse line and DNA from homozygous *sy* mice were obtained from The Jackson Laboratory, whereas *Bmp7* mutant mice were provided by Dr. L. Robertson (Harvard Medical School, Cambridge, MA) (Dudley et al., 1995).

RNA analyses

Northern blot analysis was performed on ~40 μg of total RNA purified from newborn lungs (Pereira et al., 1997); probes included the 3′ untranslated regions of *Fbn1* and *Fbn2,* and the control GAPDH (Zhang et al., 1995). In situ and whole-mount hybridizations were performed as described previously using the same *Fbn* probes (Sumiyoshi et al., 2001). Additional in situ hybridization probes included the 3′ untranslated regions of *Msx1*, *Msx2*, *Bmp-4*, and *Fgf-8* (Marazzi et al., 1997; Semba et al., 2000). RT-PCR screening of the mutant *Fbn2* transcript was performed using overlapping oligonucleotides that cover the entire gene (Zhang et al., 1995).

Immunoanalyses

The anti-Fbn1 antibody, pAb9543, was prepared using the Fbn1 NH_2-terminal half-recombinant polypeptide rF11 (Reinhardt et al., 1996). The mouse Fbn2 antibody was raised in the rabbit against the recombinant NH_2-terminal peptide rF37. The antibody was tested by ELISA against the immunizing peptide, and specificity was determined by Western blot analysis. The type II collagen monoclonal antibody was obtained from the Developmental Studies Hybridoma Bank (University of Iowa, Iowa City, IA). Western blot analyses were performed on conditioned media of primary dermal fibroblasts established from newborn *Fbn2*$^{-/-}$ and *sy*^{fp}/*sy*^{fp} mice (Gayraud et al., 2000). Antibodies were visualized with nitro blue tetrazolium/5-bromo-4-chloro-3′ indoylphosphate (Pierce Chemical Co.). For indirect immunofluorescence, fresh limbs were fixed in 2% paraformaldehyde, 0.75 M lysine, and 0.01 M sodium periodate in 1× PBS for ~4 h at 4°C, washed in 1× PBS for 1 h at 4°C, and stabilized in 40% sucrose in 1× PBS for 24 h at 4°C. The tissue was then embedded in OCT compound (Tissue Tek) and frozen in liquid nitrogen. 5 μm sections were generated using a Leica cryostat and diamond-coated disposable blades (C. L. Sturkey) and mounted on Fisherbrand Superfrost glass slides. Sections were dried at room temperature for 1 h and stored at 4°C. Immunostaining was performed as described previously (Gayraud et al., 2000), and fluorescence was monitored using a Zeiss Axiophot microscope using 10× or 20× Plan-Neofluar objective. Images were taken with a Spot camera (Diagnostic Instrument) and processed using Photoshop 5.5.

Morphological analyses

Adult mice were anesthetized by intraperitoneal injection of 0.017 ml of 25% Avitin per gram weight, and embryos were fixed in Bouin's fixative. Whole-mount pictures were taken using a Nikon SMZ-U dissecting scope and a Sony digital

photo camera (model DKC-5000); images were processed using Photoshop 5.5. For whole-mount skeletal analysis, mice were fixed overnight in 95% ethanol after removing soft tissue. Cartilage was stained in a fresh solution of 80 ml 95% ethanol, 20 ml glacial acetic acid, and 15–30 mg alcian blue (Sigma-Aldrich) for 12–48 h. Skeleton was washed twice in 95% ethanol, and soft tissue was dissolved overnight in 2% KOH. Bones were stained overnight in 1% KOH, 75 μg/ml alizarin red S (Sigma-Aldrich), destained in 20% glycerol and 1% KOH for 3–7 d, and cleared first in 20% glycerol and 20% ethanol, and then in 50% glycerol and 50% ethanol. Images were prepared as described above. X-ray radiographs were performed on anesthesized mice using a Micro 50 (Microfocus Imaging) at 30 kV for 20–30 s. In situ TUNEL assay on paraffin sections was performed using the Apoptosis Detection System (Promega).

Bead implantation

Affi-Gel blue agarose beads (Bio-Rad Laboratories) at 100–200 mesh (50–75 μm) were soaked in 100 ng/μl human recombinant BMP-4 (Genetics Institute) or in BSA, and implanted into interdigital tissue of E13.5 hindlimbs as described previously (Semba et al., 2000). After 6 h incubation at 37°C in 5% CO_2, limbs were processed for in situ hybridization.

The authors thank Drs. M. Amling, M. Baron, T. Lufkin, L. Robertson, V. Rosen, and D. Sassoon for suggestions and critical reagents, and Ms. Karen Johnson for typing the manuscript.

This work was supported by grants from the National Institutes of Health (AR42044, GM18511), the National Marfan Foundation, and the Shriners Foundation.

Submitted: 8 May 2001
Revised: 6 June 2001
Accepted: 8 June 2001

References

Chen, Y., and X. Zhao. 1998. Shaping limbs by apoptosis. *J. Exp. Zool.* 282:691–702.

Christian, J.L. 2000. BMP, Wnt and Hedgehog signals: how far can they go? *Curr. Opin. Cell Biol.* 12:244–249.

Dahna, R.D., and J.F. Fallon. 2000. Interdigital regulation of digit identity and homeotic transformation by modulated BMP signaling. *Science.* 289:438–441.

Dudley, A.T., Lyons K.M., and Robertson E.J. 1995. A requirement for bone morphogenetic protein-7 during development of the mammalian kidney and eye. *Genes Dev.* 9:2795–2807.

Flaumenhaft, R., and D.B. Rifkin. 1991. Extracellular matrix regulation of growth factor and protease activity. *Curr. Opin. Cell Biol.* 3:817–823.

Ganan, Y., D. Macias, M. Duturque-Cocquilland, and J.M. Hurlé. 1996. Role of TGFβ and BMPs as signals controlling the position of the digits and the areas of interdigital cell death in the developing chick limb autopod. *Development.* 122:2349–2357.

Ganan, Y.D., Macias, R.D. Basco, R. Merino, and J.M. Hurlé. 1998. Morphological diversity of the avian foot is related with the pattern of *msx* gene expression in the developing autopod. *Dev. Biol.* 196:33–41.

Gayraud, B., D.R. Keene, L.Y. Sakai, and F. Ramirez. 2000. New insights into the assembly of extracellular microfibrils from the analysis of the fibrillin 1 mutation in the tight skin mouse. *J. Cell Biol.* 150:667–680.

Handford, P.A., A.K. Downing, D.P. Reinhardt, and L.Y. Sakai. 2000. Fibrillin: from domain structure to supramolecular assembly. *Matrix Biol.* 19:457–470.

Hertwig, P. 1942. Neue mutationen und koppelungsgruppen bei der hausmaus. *Z. Induklt. Abstammungs Vererbungsl.* 80:220–246.

Hogan, B.M.L. 1996. Bone morphogenetic proteins: multifunctional regulators of vertebrate development. *Genes Dev.* 10:1580–1594.

Hurlé, J.M., G. Corson, K. Daniels, R.S. Reiter, L.Y. Sakai, and M. Solursh. 1994. Elastin exhibits a distinctive temporal and spatial pattern of distribution in the developing chick limb in association with the establishment of the cartilaginous skeleton. *J. Cell Sci.* 107:2623–2634.

Johnson, K.R., S.A. Cook, and Q.Y. Zheng. 1998. The original shaker-with-syndactylism mutation (sy) is a contiguous gene deletion syndrome. *Mamm. Genome.* 9:889–892.

Johnson, R.L., and C.J. Tabin. 1997. Molecular models for vertebrate limb development. *Cell.* 90:979–990.

Lane, P.W., and K.P. Hummel. 1973. Fused phalanges allelic with sy. *Mouse News Letter.* 49:32.

Lane, P.W., A.G. Searle, C.V. Beechey, and E. Eicher. 1981. Chromosome 18 of the house mouse. *J. Hered.* 72:409–412.

Li, X., L. Pereira, H. Zhang, C. Sanguineti, F. Ramirez, J. Bonadio, and U. Francke. 1993. Fibrillin genes map to regions of conserved mouse/human synteny mouse chromosomes 2 and 18. *Genomics.* 18:667–672.

Luo, G., C. Hofmann, A.L.J.J. Bronckers, M. Sohocki, A. Bradlery, and G. Karsenty. 1995. BMP-7 is an inducer of nephrogenesis, and is also required for eye development and skeletal patterning. *Genes Dev.* 9:2808–2820.

Macias, D., Y. Ganan, T.K. Sampath, M.E. Piedra, M.A. Ros, and J.M. Hurlé. 1997. Role of BMP-2 and OP-1 (BMP-7) in programmed cell death and skeletogenesis during chick limb development. *Development.* 124:1109–1117.

Marazzi, G., Y. Wang, and D. Sassoon. 1997. Msx2 is a transcriptional regulator in the BMP4-mediated programmed cell death pathway. *Dev. Biol.* 186:127–138.

Mecham, R.P., and E. Davis. 1994. Elastic fiber structure and assembly. *In* Extracellular Matrix Assembly and Structure. P.D. Yurchenco, D.E. Birk, and R.P. Mecham, editors. Academic Press, New York. 281–314.

Merino, R., Y. Ganan, D. Macias, A.N. Economides, K.T. Sampath, and J.M. Hurlé. 1998. Morphogenesis of digits in the avian limb is controlled by FGFs, TGFβs, and Noggin through BMP signaling. *Dev. Biol.* 200:35–45.

Merino, R., J. Rodriguez-Leon, D. Macias, Y. Ganan, A.N. Economides, and J.M. Hurlé. 1999. The BMP antagonist Gremilin regulates outgrowth, chondrogenesis and programmed cell death in the developing limb. *Development.* 126:5515–5522.

Pereira, L., K. Andrikopoulos, J. Tian, S.Y. Lee, D.R. Keene, R. Ono, D.P. Reinhardt, L.Y. Sakai, N.J. Biery, T. Bunton, H.C. Dietz, and F. Ramirez. 1997. Targeting of the gene encoding fibrillin-1 recapitulates the vascular aspect of Marfan syndrome. *Nat. Genet.* 17:218–222.

Pereira, L., S.Y. Lee, B. Gayraud, K. Andrikopoulos, S.D. Shapiro, T. Bunton, N.J. Biery, H.C. Dietz, L.Y. Sakai, and F. Ramirez. 1999. Pathogenetic sequence for aneurysm revealed in mice underexpressing fibrillin-1. *Proc. Natl. Acad. Sci. USA.* 96:3819–3823.

Ramirez, F. 1996. Fibrillin mutations in Marfan syndrome and related phenotypes. *Curr. Opin. Genet. Dev.* 6:309–315.

Reinhardt, D.P., D.R. Keene, G.M. Corson, E. Poschl, H.P. Bachinger, J.E. Gambee, and L.Y. Sakai. 1996. Fibrillin-1: organization in microfibrils and structural properties. *J. Mol. Biol.* 258:104–116.

Semba, I., K. Nonaka, I. Takahashi, K. Takahashi, R. Dashner, L. Shum, G.H. Nuckolls, and H.C. Slavkin. 2000. Positionally-dependent chondrogenesis induced by BMP4 is co-regulated by Sox9 and Msx2. *Dev. Dyn.* 217:401–414.

Sumiyoshi, H., F. Laub, H., Yoshioka, and F. Ramirez. 2001. Embryonic expression of type XIX collagen is transient and confined to muscle cells. *Dev. Dyn.* 220:155–162.

Sweet, H.O. 1996. Remutations at The Jackson Laboratory. *Mouse Genome.* 94: 487.

Tang, M.K., A.K.C. Leung, W.H. Kwong, P.H. Chow, P.H. Chan, V. Ngo-Muller, M. Li, and K.K.H Lee. 2000. Bmp-4 requires the presence of digits to initiate programmed cell death in limb interdigital tissues. *Dev. Biol.* 218: 89–98.

Taipale, J., and J. Keski-Oja. 1997. Growth factors in the extracellular matrix. *FASEB J.* 11:51–59.

Tickle, C. 1999. Morphogen gradients in vertebrate limb development. *Semin. Cell Dev. Biol.* 10:345–351.

Yang, Q., K. Ota, Y. Tian, A. Kumar, J. Wada, N. Kashihara, E. Wallner, and Y.S. Kanwar. 1999. Cloning of rat fibrillin-2 cDNA and its role in branching morphogenesis of embryonic lung. *Dev. Biol.* 212:229–242.

Zhang, H., W. Hu, and F. Ramirez. 1995. Developmental expression of fibrillin genes suggests heterogeneity of extracellular microfibrils. *J. Cell Biol.* 129: 1165–1176.